

Fault Detection in Rotating Machinery:

vibration analysis and numerical modeling

Ali Moshrefzadeh

Ph.D candidate, 30° cycle

Prof. Alessandro Fasana

Supervisor



Planetary Gears are Widely Used:

- Aerospace
- Wind Turbines
- Automotive

❖ Project Objectives

- Investigate the Vibration Properties of Planetary Gearboxes
- Diagnosis of Bearings and Gears

❖ Mathematical Model

- A Good Understanding Of Structure Dynamic Characteristics
- Reasonably Accurate
- Suitable For Evaluations During Design Stages
- Flexible

Advantage:

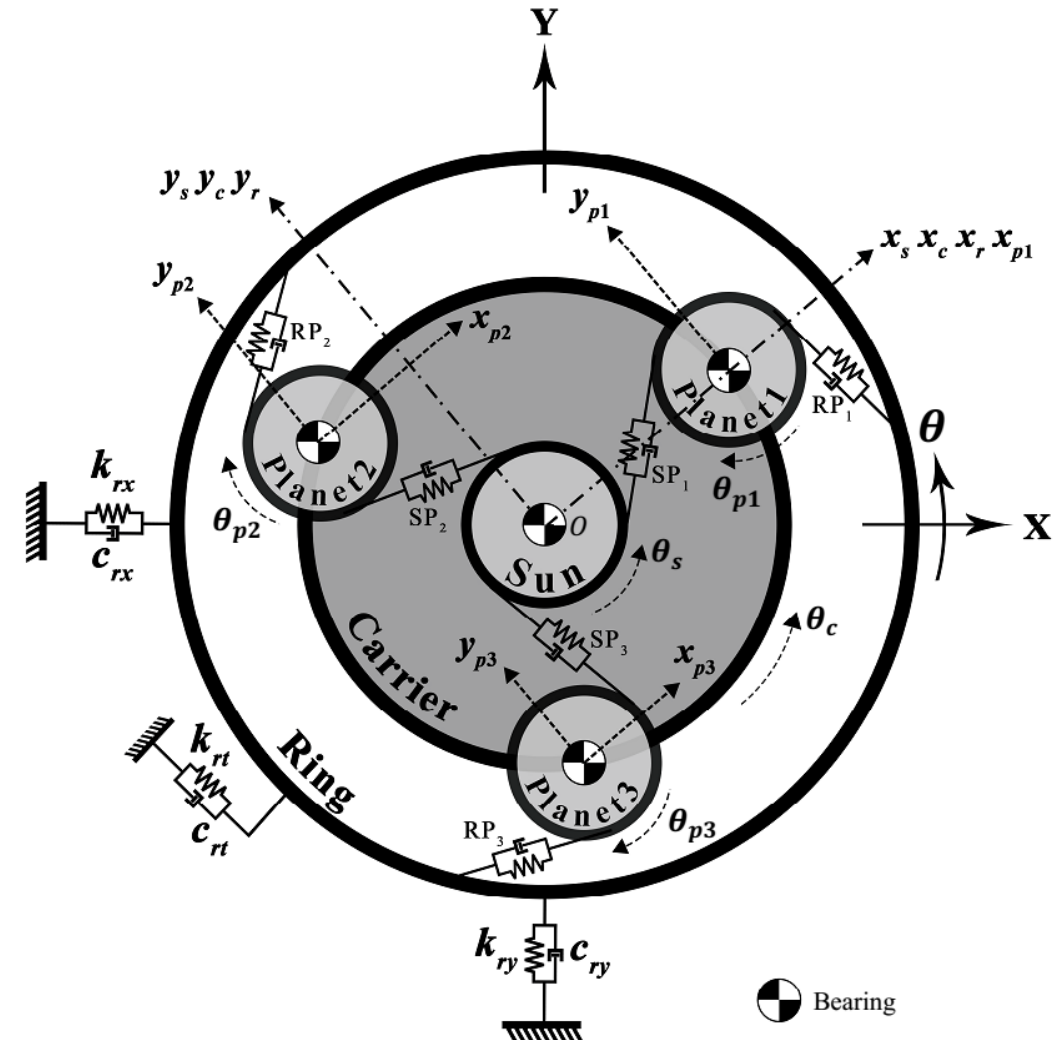
- Compactness
- High Torque-to-Weight Ratios
- Multiple Gear Ratios

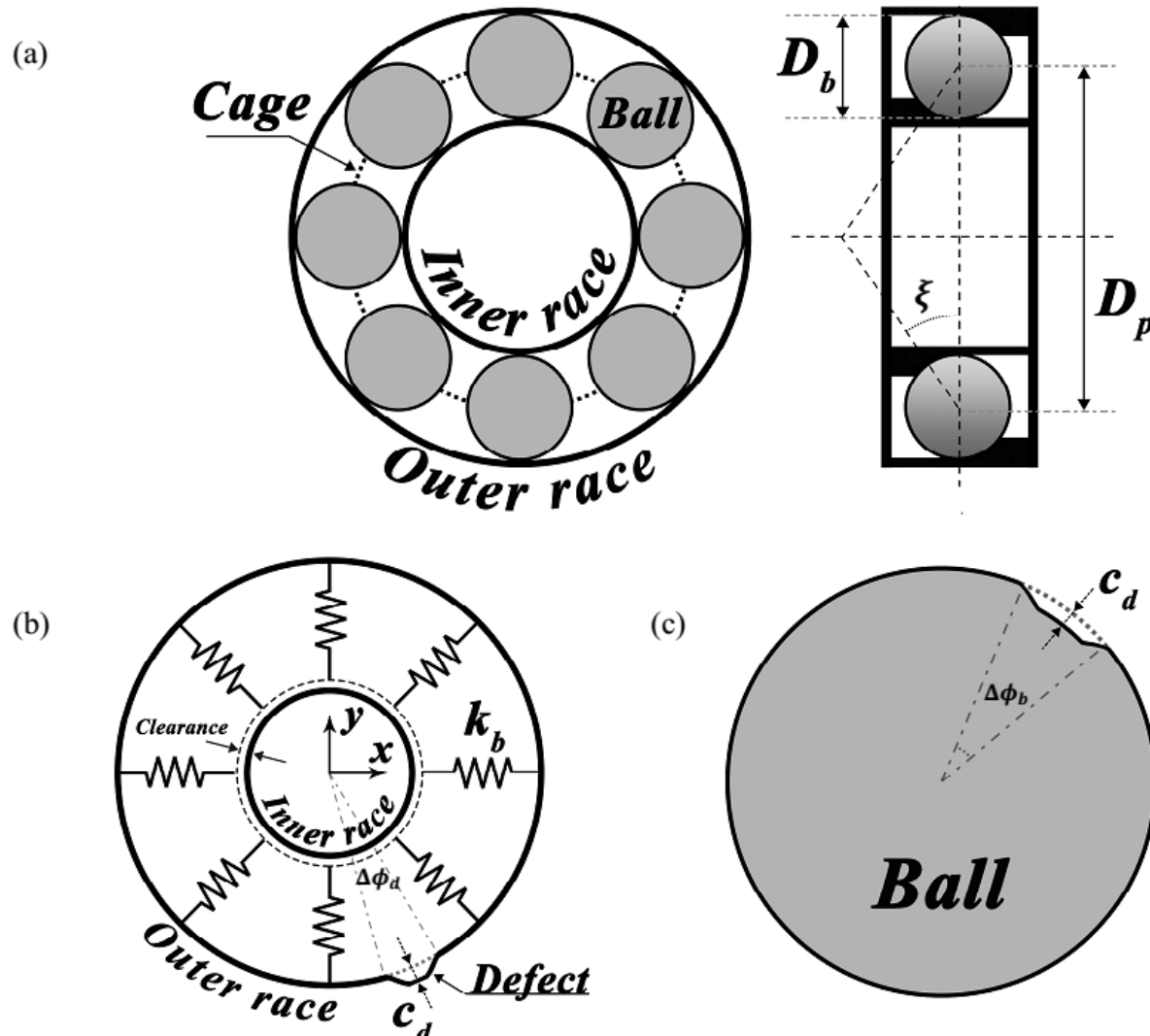


- Each Gear and the Carrier are Considered as Rigid Bodies with Three DOFs
- The Flexible Gear Teeth Contacts are Modelled by Springs and Dampers
- Comprehensive Bearing Model

❖ Time-Varying Mesh Stiffness

- Number of Teeth Pairs in Contact Change
- Contact Positions of Gear Teeth Alter
- One of the Main Sources of Vibration
- It is calculated by Potential Energy Method





- Four Degrees of Freedom
- Flexibility of Rollers: Circumferentially Distributed Radial Springs
- Hertzian Contact Between Balls/Rollers and Races are Assumed

$$F_j = k_b \delta_j^n$$

$n = 1.5$ for ball bearings and 1.1 for roller bearings

- Overall Bearing Stiffness Varies

❖ Localized Fault Modeling

- Variation of Balls Force Inside the Defected Region
- This Variation Can Be Utilized to Detect Defects

Summarizing the model



- Capacity of Modelling Cracks and Spalls of Gears and Bearings with different sizes, locations and profiles
- Time Varying Gear Mesh and Bearing Stiffness
- Nonlinear Bearing Stiffness

Equations of Motion

- 18 Degrees of Freedom

The Sun Gear Equations of Motion

$$m_s \ddot{x}_s + F_{sbx} + \sum_{n=1}^N F_{spn} \cos \Psi_{sn} = m_s \dot{x}_s^2 + 2m_s \dot{y}_s \dot{\theta}_c + m_s y_s \ddot{\theta}_c,$$

$$m_s \ddot{y}_s + F_{sby} + \sum_{n=1}^N F_{spn} \sin \Psi_{sn} = m_s \dot{y}_s^2 - 2m_s \dot{x}_s \dot{\theta}_c - m_s x_s \ddot{\theta}_c,$$

$$\left(\frac{J_s}{r_s} \right) \ddot{\theta}_c + \sum_{n=1}^N F_{spn} = \frac{T_i}{r_s},$$

- Rotating Gear Frames

F_{spn} represents the gear mesh force

$$F_{spn} = k_{spn} \delta_{spn} + c_{spn} \dot{\delta}_{spn},$$

$$\delta_{spn} = (x_s - x_{pn}) \cos \Psi_{sn} + (y_s - y_{pn}) \sin \Psi_{sn} + r_s \theta_s + r_p \theta_{pn} - r_c \theta_c \cos \alpha,$$

F_{sbx} and F_{sby} represent the sun bearing force in x_s and y_s directions

$$F_{sbx} = c_{sx} \dot{x}_s + k_b \sum_{j=1}^{N_b} \gamma_j \left[x_s \cos \phi_{sj} + y_s \sin \phi_{sj} - \beta_j C_d - c \right]^{1.5} \cos \phi_{sj}$$

$$F_{sby} = c_{sy} \dot{y}_s + k_b \sum_{j=1}^{N_b} \gamma_j \left[x_s \cos \phi_{sj} + y_s \sin \phi_{sj} - \beta_j C_d - c \right]^{1.5} \sin \phi_{sj}$$

$$\phi_{sj} = \frac{2\pi(j-1)}{N_b} + \frac{\theta_s}{2} \left(1 - \frac{D_b}{D_p} \cos \xi \right) + \phi_0 - \theta_c$$

These Coupled Nonlinear and Time Variant ODE Are Numerically Solved to Calculate the Ring Gear Acceleration Signal

❖ Planet-Bearing

- Exhibit a High Failure Rate
- Transmit the Torque From Input of the System to the Output

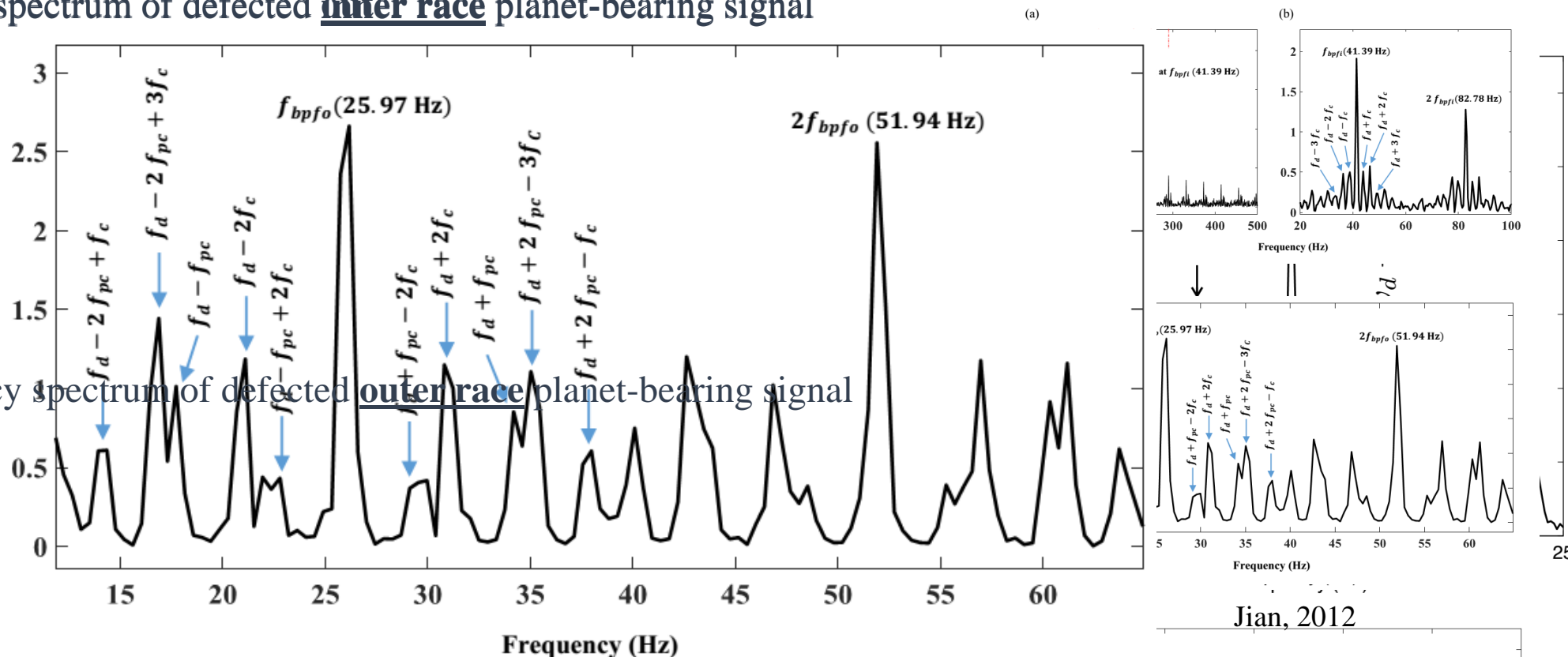
❖ Frequency Analysis of Defect Signals

- Faulty Inner Race, Outer Race and Rolling Element
- Residual Signals: Difference Between the Time Responses of Damaged and Undamaged Systems

Frequency Analysis of Defect Signals



❖ Frequency spectrum of defected inner race planet-bearing signal

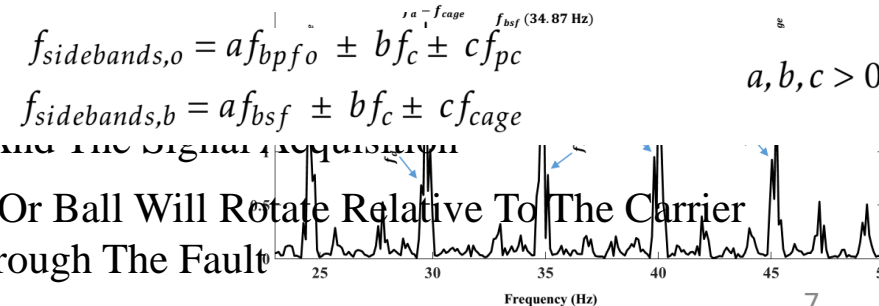


❖ Frequency spectrum of defected outer race planet-bearing signal

Cluster Of Sidebands:

Cluster Of Sidebands:

- Carrier Rotation (f_c)
- Relative Rotation Between The Transmission Path Between The Planet-bearing And The Signal Acquisition
- Force Which Is Caused By The Defective Planet-bearing Outer Race Or Ball Will Rotate Relative To The Carrier
- Ball/Roller May Lose Its Contact With The Races While It Passes Through The Fault
- Angle Between The Defect Force And Ring-planet Mesh Varies

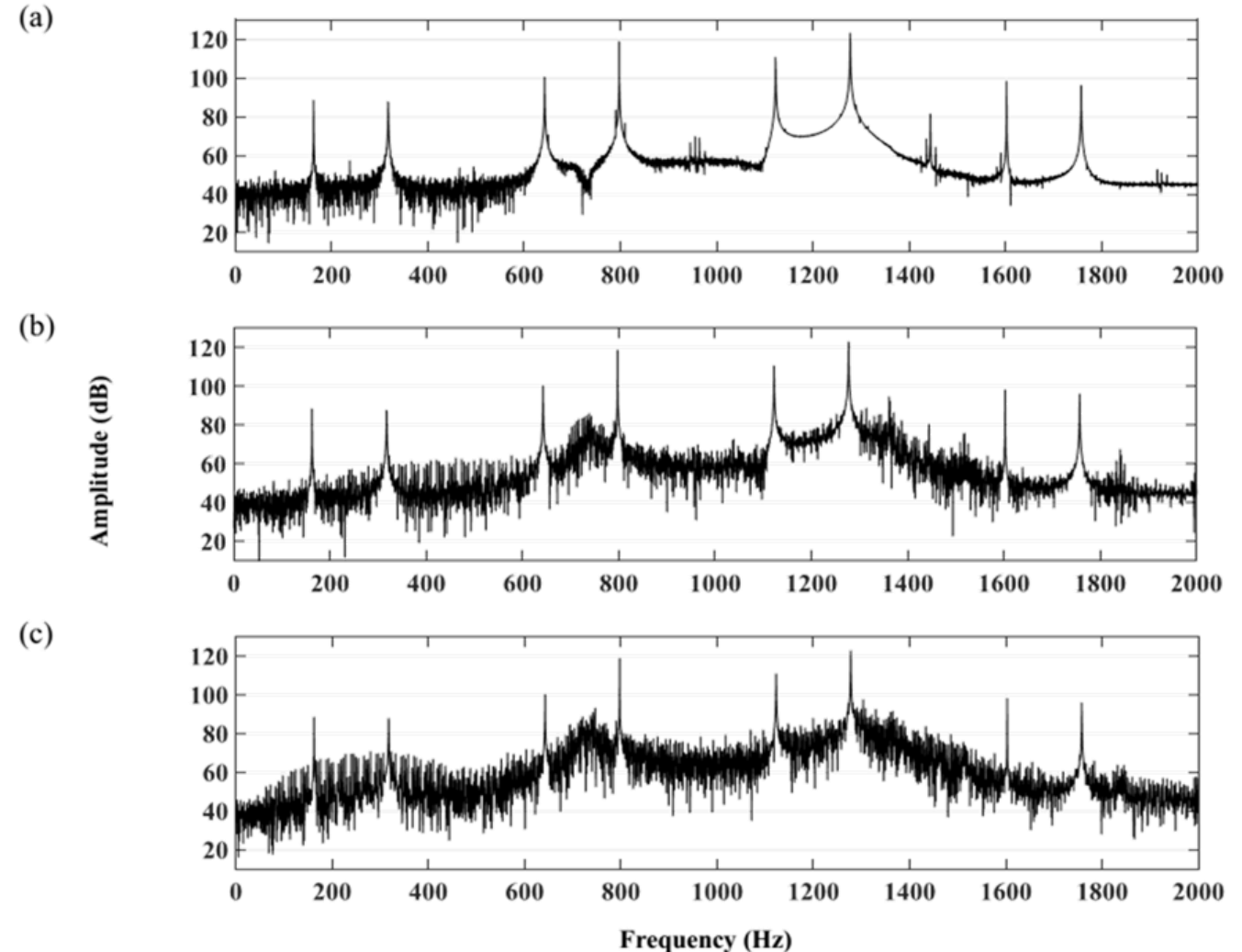


Jian, 2012

Frequency Spectrum of the Ring Acceleration Signals



- Healthy and Defected Planet Bearing
- Sidebands Emerge When Defect Is Present
 - Combination Of BPF and Its Sidebands
- Amplitudes of Meshing Frequency and Its Harmonics are Not Affected by Faults
- Amplitudes of Sidebands Increase as the Size of Spall Grows
- These Variations are Believed to be Worthwhile for Fault Diagnosis of Planetary Gearboxes

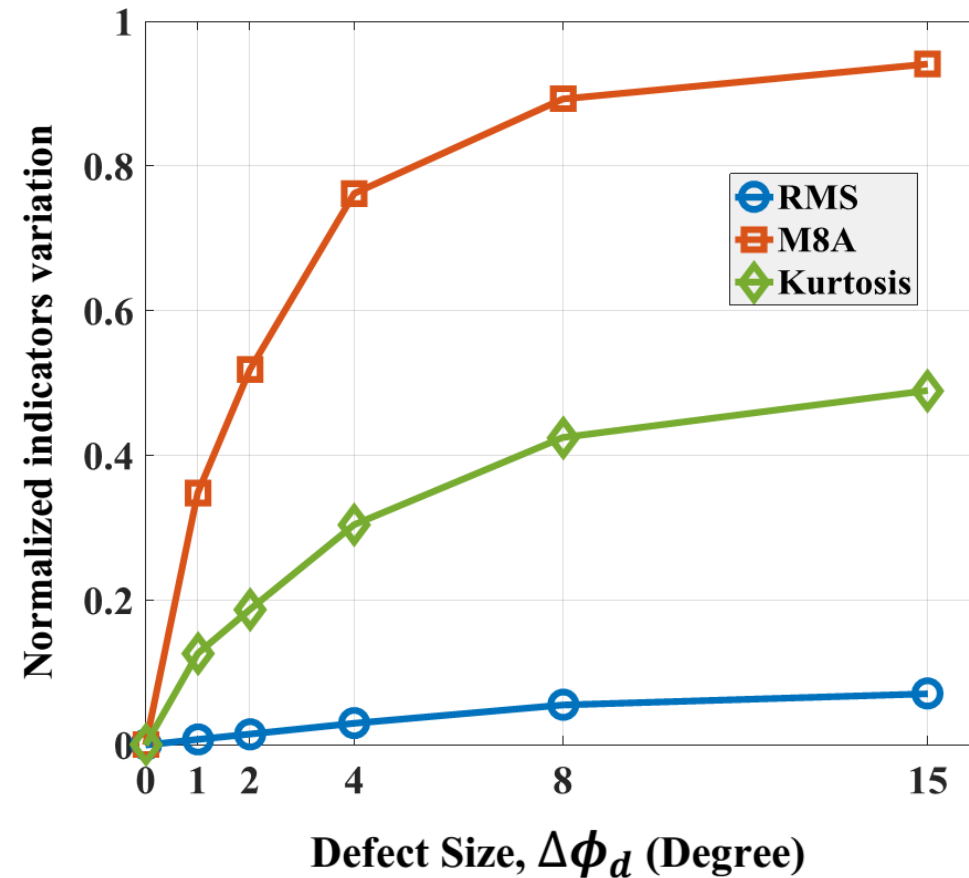


(a) healthy gearbox (b) defected planet inner race, $\Delta\varphi_d = 2^\circ$ and (c) 4°

Condition Monitoring of the Gearbox



- Statistical Features are Usually Used as an Indicator of Bearings and Gears Faults Presence and Growth
 - RMS
 - Kurtosis
 - M8A
- Condition Indicators for 5 Defect Cases
- All The Statistical Indicators Quantities Rise with the Growth of the Planet's Defect Size
- M8A Indicator is More Sensitive to the Presence of the Defects
 - Potential to Diagnose Spalls Even in Their Emerging Stages



Rolling Element Bearings

Bearings Localized defects

- (a) Outer race
- (b) Inner race
- (c) Rolling element



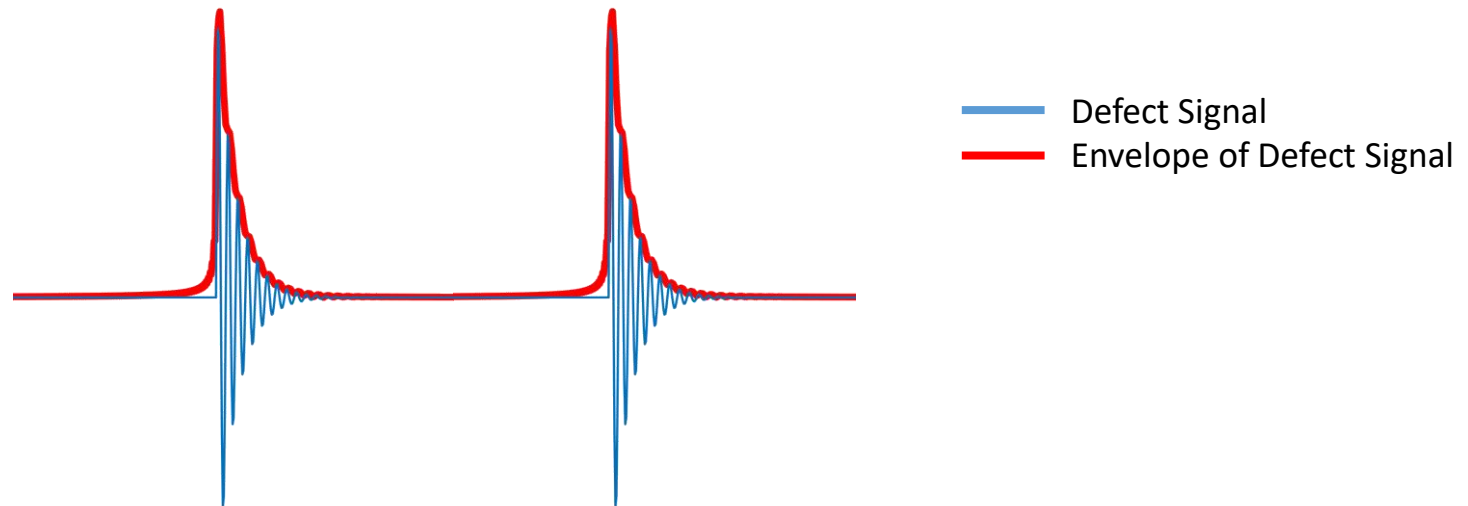
- One of the most widely element in rotating machinery
- Their failure is the most important cause of machinery breakdowns
- Correctly detecting and diagnosing bearing faults at stages prior to their complete failure is crucial

* Li, K., Ping, X., Wang, H., Chen, P. and Cao, Y., 2013. Sequential fuzzy diagnosis method for motor roller bearing in variable operating conditions based on vibration analysis. *Sensors*, 13(6), pp.8013-8041

Avoids potential catastrophic damage not only to the apparatus but also to the personnel

Vibration Based Diagnosis:

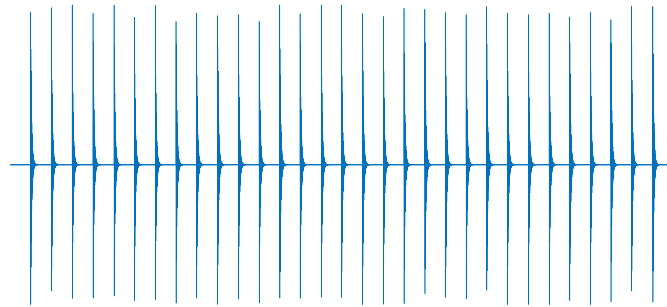
- **Localized defects:** an impact is generated each time the defect is engaged and consequently the bearing and machine structure are excited



- **Envelope analysis:** has been used for long time to extract the bearing defect frequencies

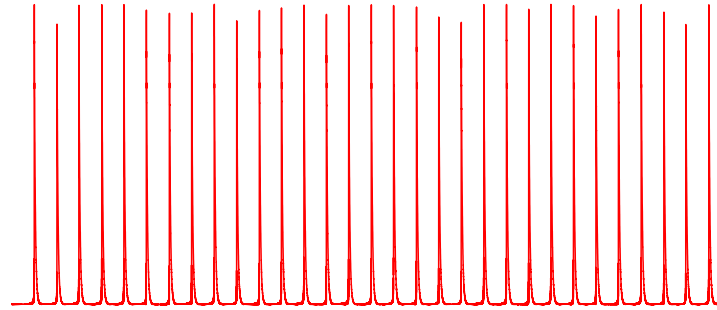
Rolling Element Bearings

Time signal



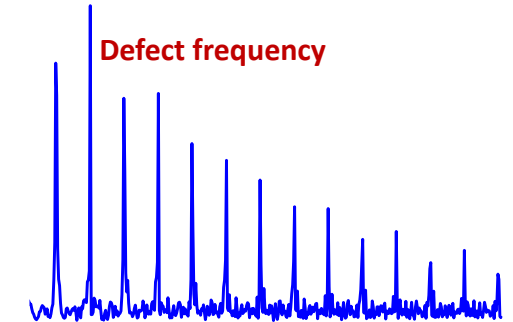
t (sec)

Envelope signal



t (sec)

Frequency Domain



f (Hz)

- Ballpass frequency, outer race (BPFO):

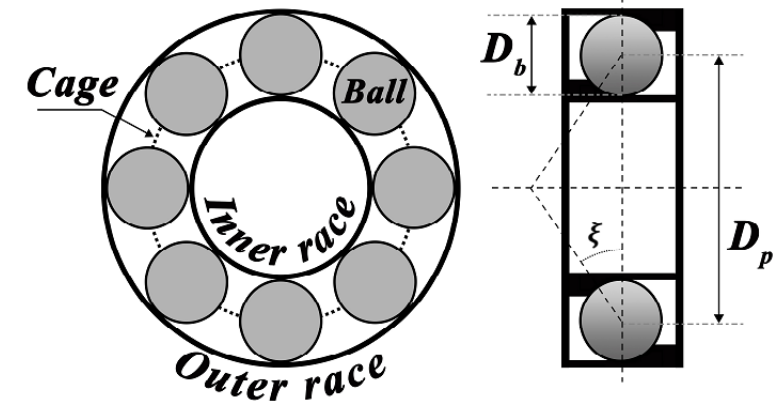
$$f_{bpfo} = \frac{N_b}{2}(f_o - f_i)\left(1 - \frac{D_b}{D_p}\cos\xi\right)$$

- Ballpass frequency, inner race (BPFI):

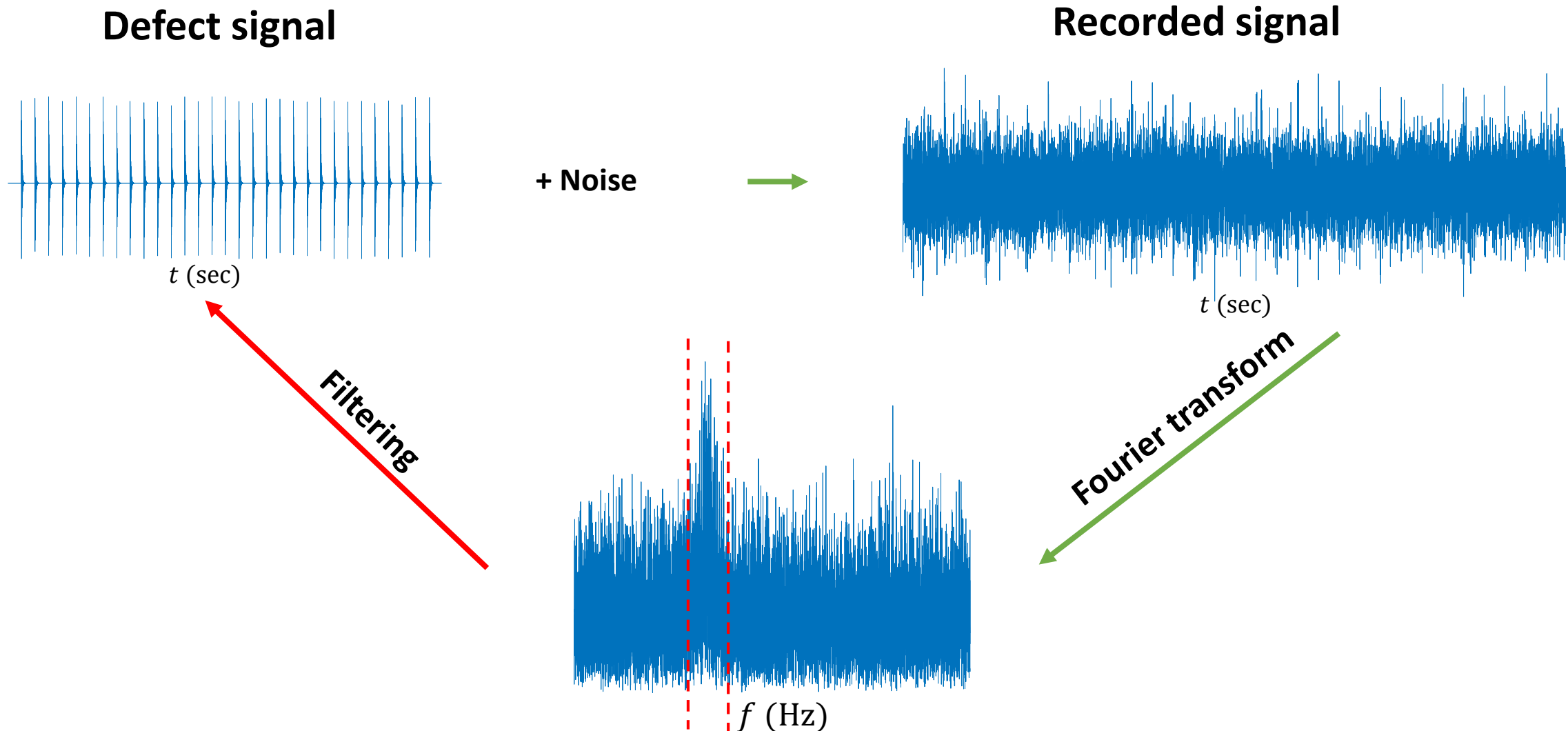
$$f_{bpfi} = \frac{N_b}{2}(f_o - f_i)\left(1 + \frac{D_b}{D_p}\cos\xi\right)$$

- Ball (roller) spin frequency (BSF):

$$f_{bsf} = \frac{f_o - f_i}{2} \frac{D_p}{D_b} \left(1 - \left(\frac{D_b}{D_p}\cos\xi\right)^2\right)$$



Introduction

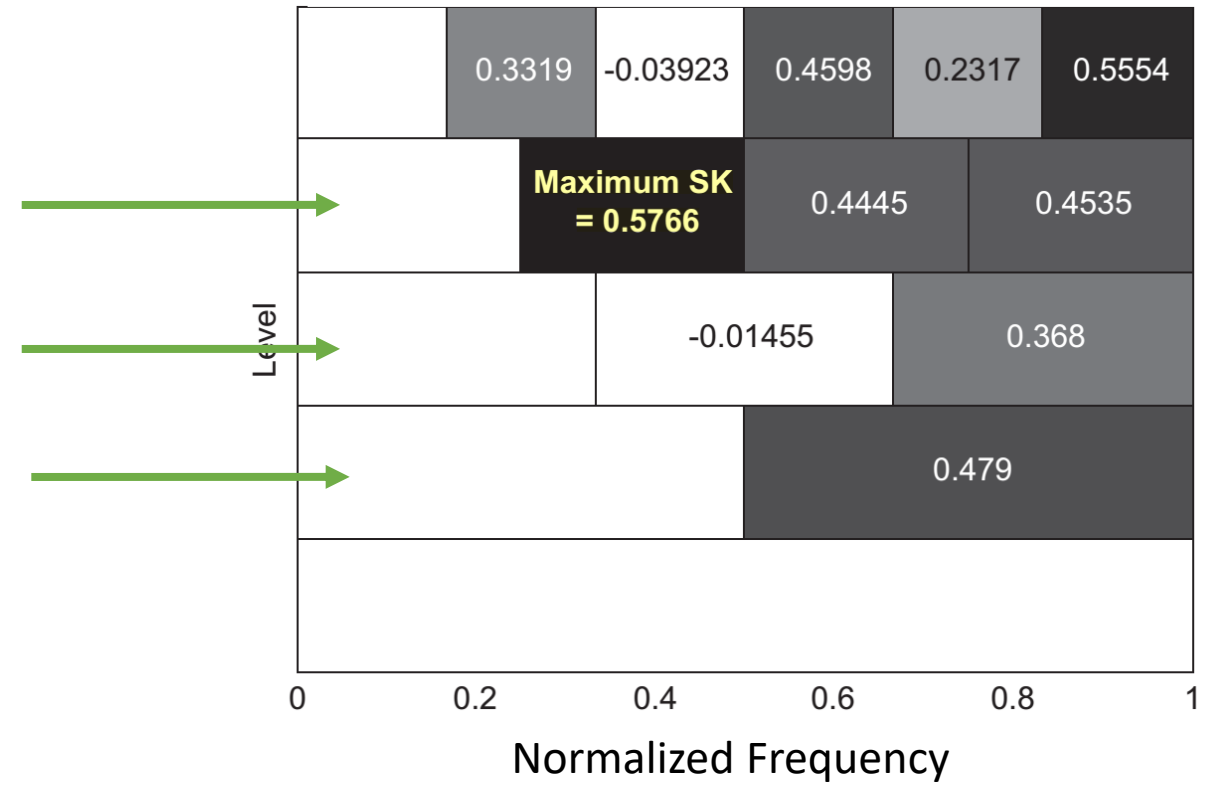
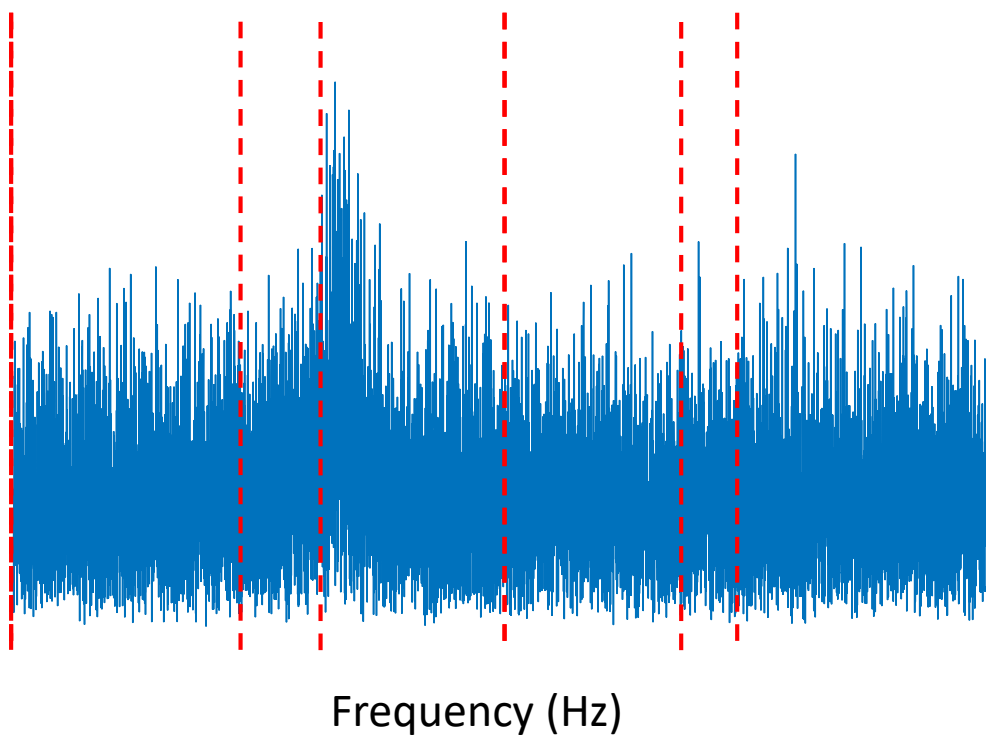


- **Main challenge:** finding the most suitable frequency band for demodulation

Spectral kurtosis and Kurtogram



- **Spectral kurtosis (SK)** has been a significant step to unravel this problem
 - Find the most impulsive frequency band



Quantify the impulsivity:
$$\text{Kurtosis} = \frac{\sum x_i^4}{[\sum (x_i^2)]^2}$$

Proposed Method

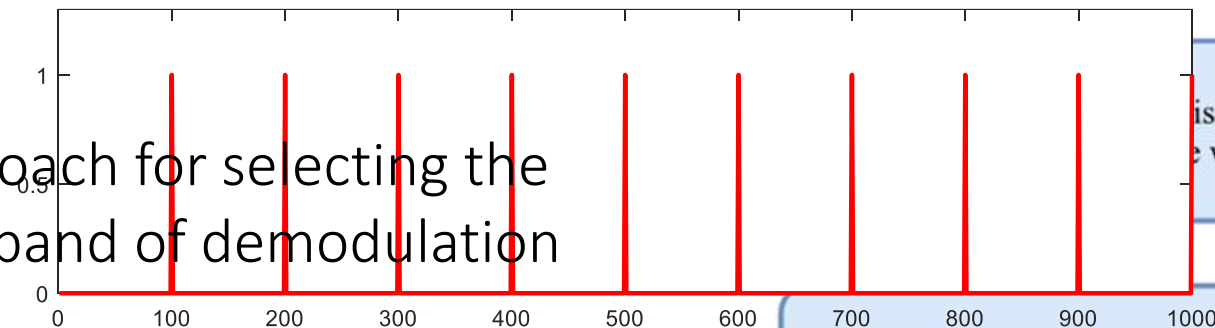
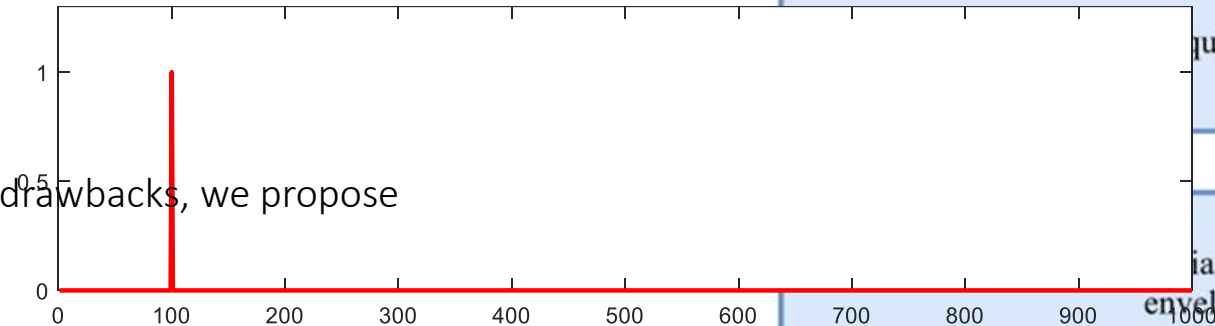


Fast Kurtogram is vulnerable to impulsive noise which makes it more sensible to individual impulses than to series of transients

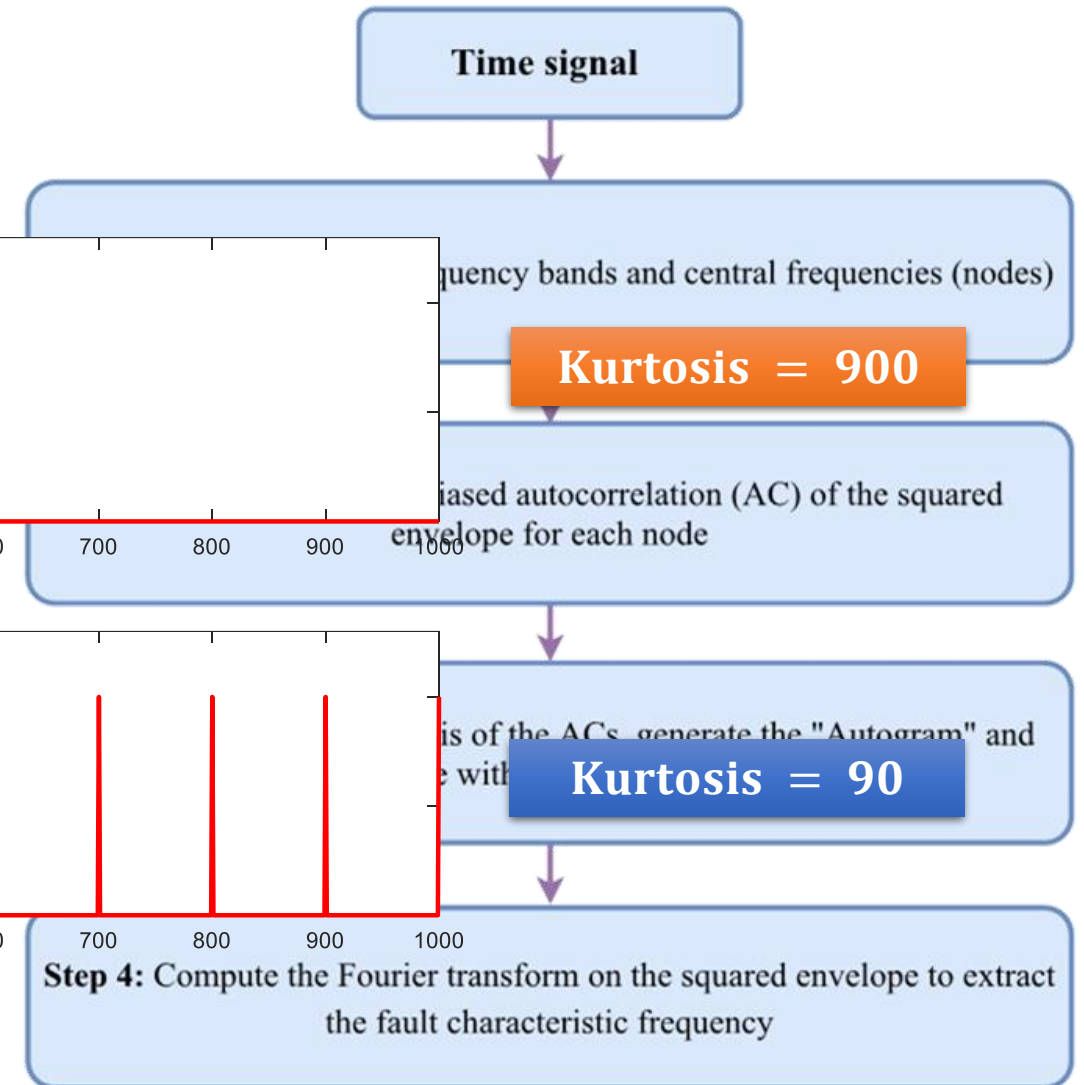
To overcome the mentioned drawbacks, we propose

Autogram:

An alternative approach for selecting the optimal frequency band of demodulation



Flowchart of the proposed method in 4 steps



- **Maximal overlap discrete wavelet packet transform (MODWPT)**
 - Split a signal in different frequency bands and central frequencies (node)
- **Differences with discrete wavelet packet transform (DWPT)**
 - Down-sampling step in DWPT is removed
 - at higher levels the lengths of the coefficient series are much shorter which causes larger estimation error
 - DWPT can be sensitive to the selection of starting point
 - Full length of signal is needed to implement the next steps

Step 2



- **Cyclostationary of order n**

- n th order statistics is periodic

$$R_{xx}(t, \tau) = \mathbf{E}\{x(t - \tau/2)x(t + \tau/2)\}$$

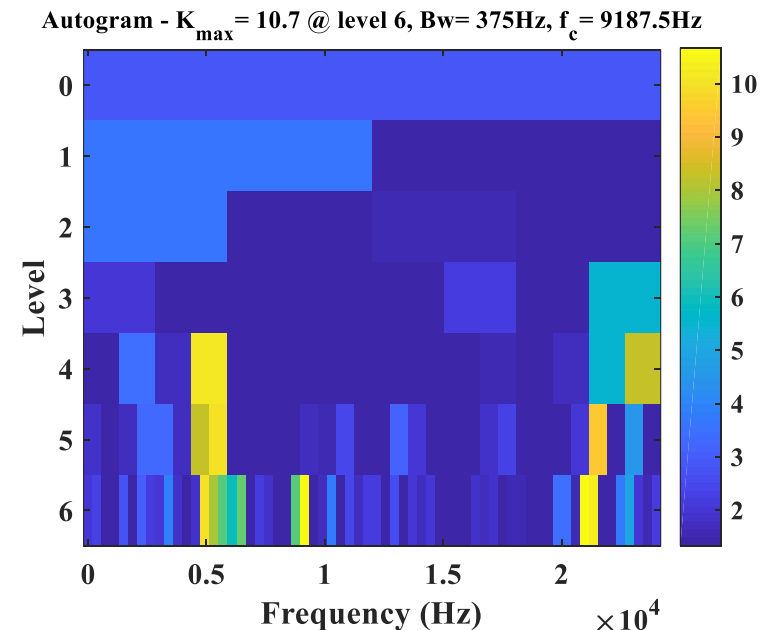
$$R_{xx}(t, \tau) = R_{xx}(t + T, \tau),$$

- **Bearing localized faults show high level of 2nd order cyclostationary**
- **Fundamental motivation of this work is to take advantage of this periodicity**
 - instantaneous autocovariance of the signal is periodic (similarly the envelope signal)
 - *unbiased AC* is performed on the squared envelope of the filtered signal for each node
- **This step has the benefits:**
 1. Decreasing the noise level
 2. Removing the random impulsive content and enhancement of periodic part of the signal

Step 4



- **Goal of this step**
 - find the most suitable frequency band for demodulation
 - a proper selection is substantial to have a successful diagnosis
- **Fourier transform** is performed on **envelope** of the filtered signal
- **Autogram**
 - Calculate the kurtosis value of the signals resulting from step 2 (unbiased autocorrelation of the squared envelope)
 - Diagnose type of the faults
 - All kurtosis values, similar to Kurtogram, are presented in a colormap
 - Node with the highest kurtosis is considered for further computation

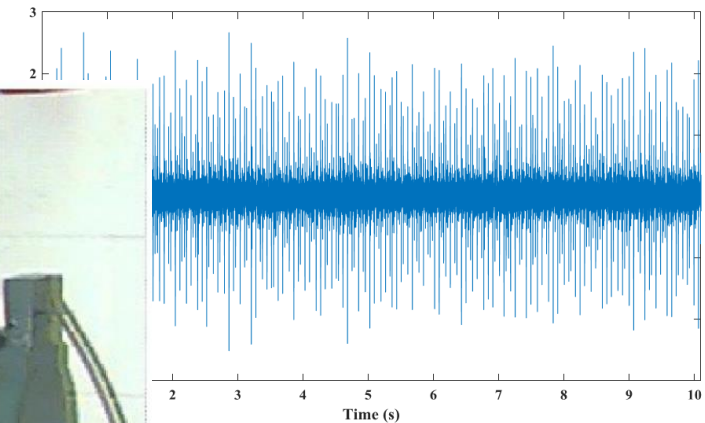
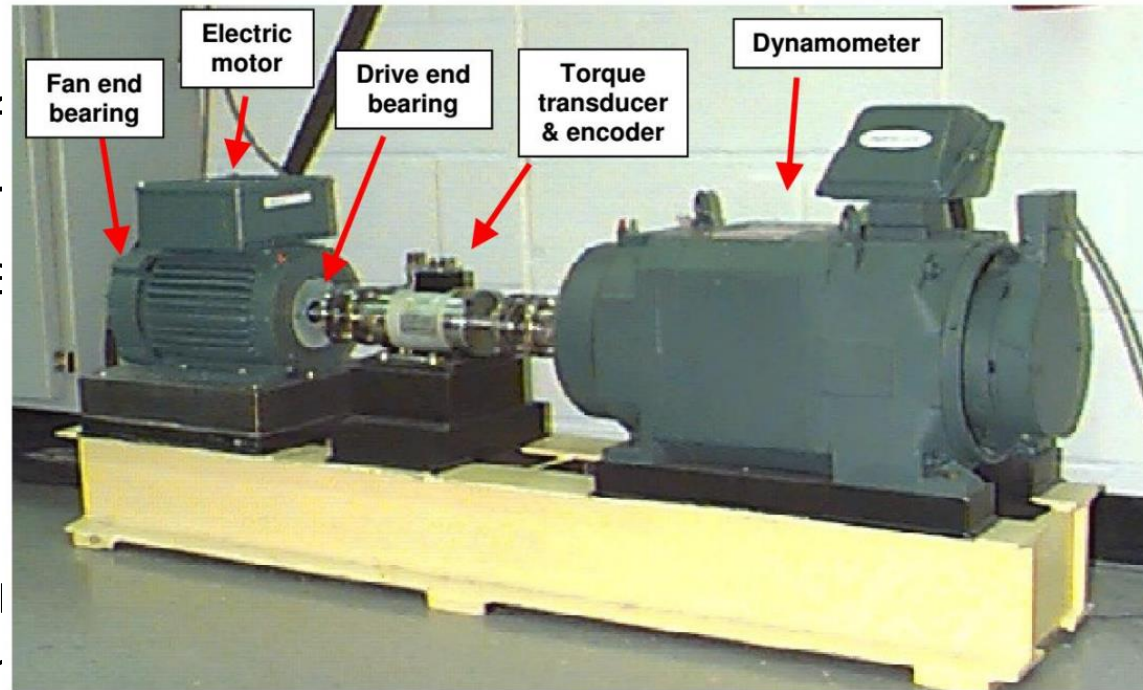


Results and Discussion

- Two data sets provided by the Case Western Reserve University (CWRU) Bearing Data Center as a standard reference

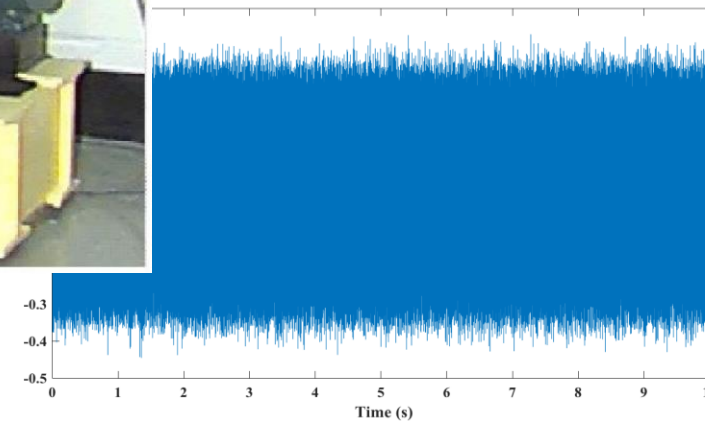
Case 1:

- Inner race def
- Many defect r
the time wave



Case 2:

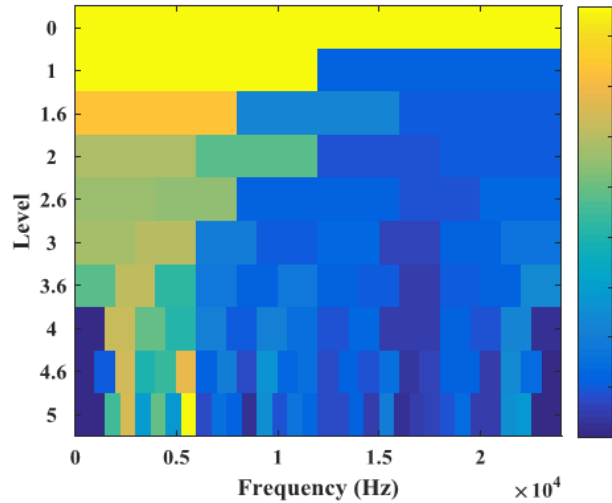
- Rolling element
- No defect trar
waveform



Autogram: Case 1

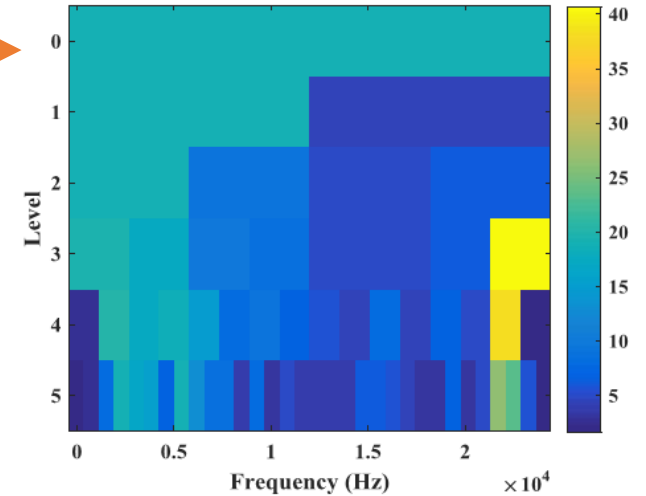


Fast Kurtogram - $K_{\max} = 17.2$ @ level 5, Bw= 750Hz, $f_c = 5625$ Hz



← **Fast Kurtogram** vs **Autogram** →

Autogram - $K_{\max} = 40.6683$ @ level 3, Bw= 3000Hz, $f_c = 22500$ Hz

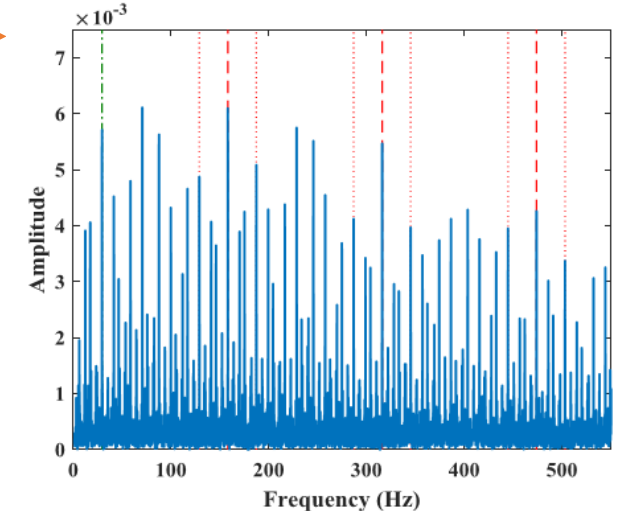
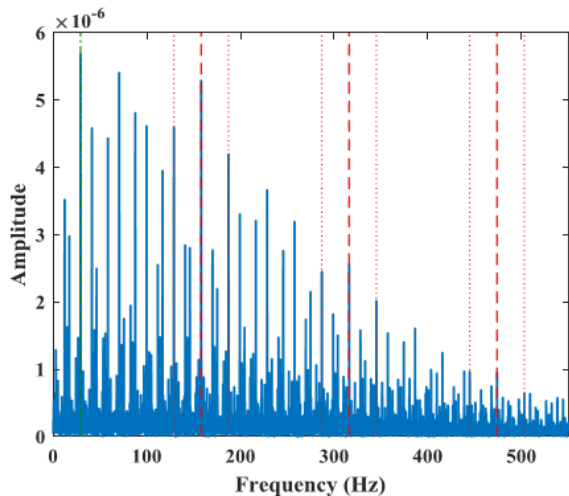


5	Level	3
5625 Hz	Center frequency	22500 Hz
750 Hz	Bandwidth	3000 Hz

← **squared envelope spectrum of the filtered signals** →

Red dash-dot line: nominal defect frequency

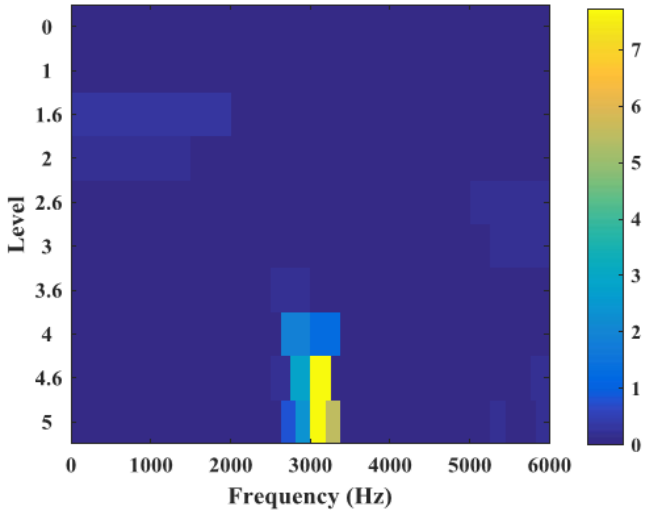
- Different demodulation band
- Successful diagnosis for both method
- Fast Kurtogram selected node also have high kurtosis in the Autogram
- Autogram selected node is not clearly detectable in the Fast Kurtogram



Autogram: Case 2

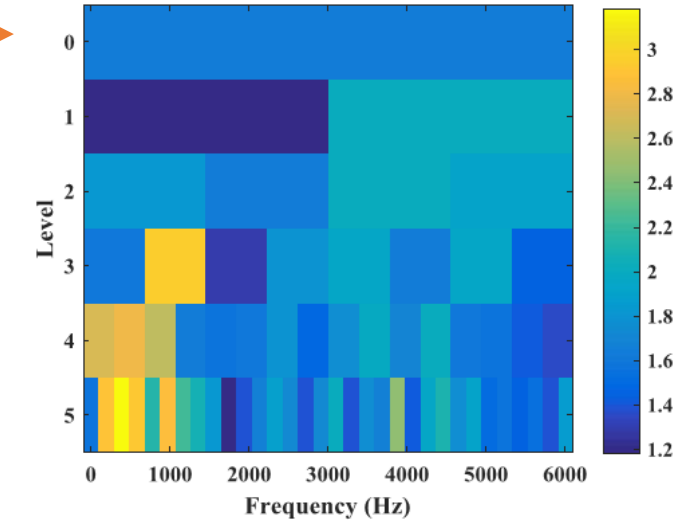


Fast Kurtogram - $K_{\max}=7.7$ @ level 4.5, Bw= 250Hz, $f_c=3125$ Hz

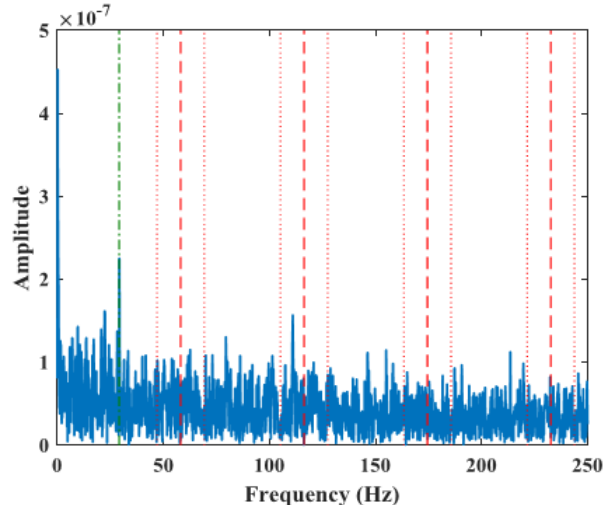


← **Fast Kurtogram** vs **Autogram** →

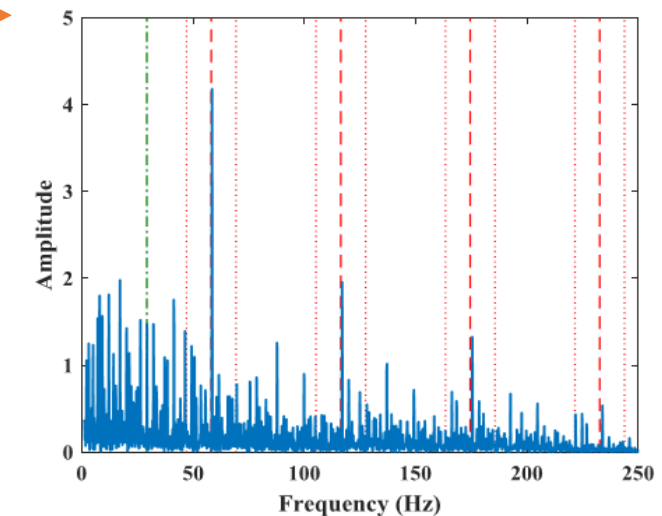
Autogram - $K_{\max}=3.1841$ @ level 5, Bw= 187.5Hz, $f_c=468.75$ Hz



squared envelope spectrum of the filtered signals



- Fast Kurtogram does not detect the bearing fault
- Autogram: harmonics of ball spin frequency (BSF) can be detected
- Another frequency band can be identified in the right side of the Autogram
- Frequency band associated to the impulsive noise has lower kurtosis value in Autogram



Autogram: Case 2



Filtered signal associated with the node with the highest kurtosis in the

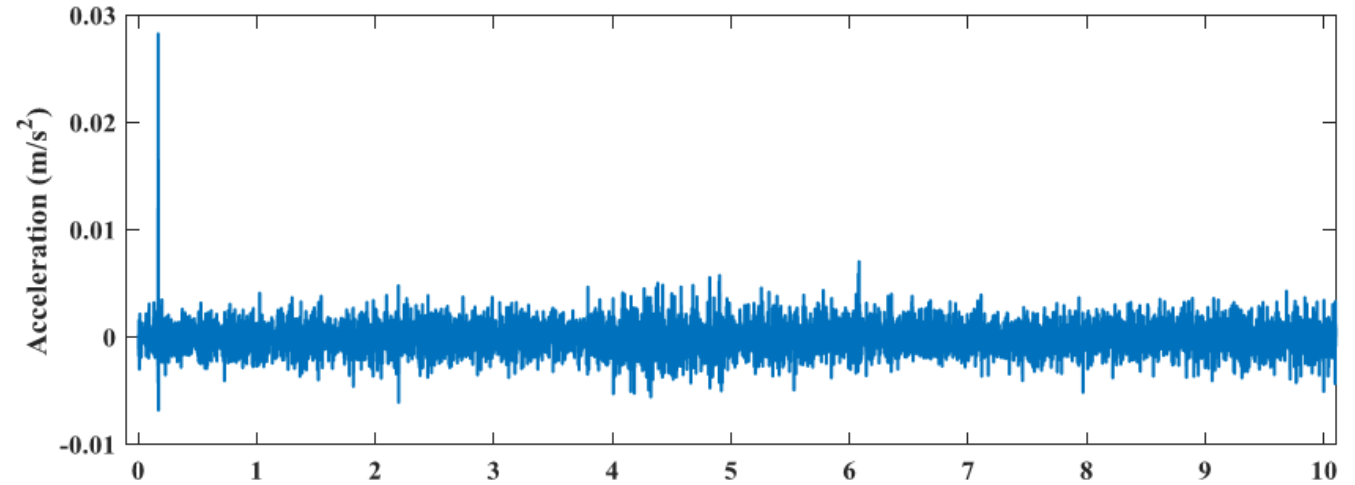
(a) Fast Kurtogram

- vulnerable to impulsive noise

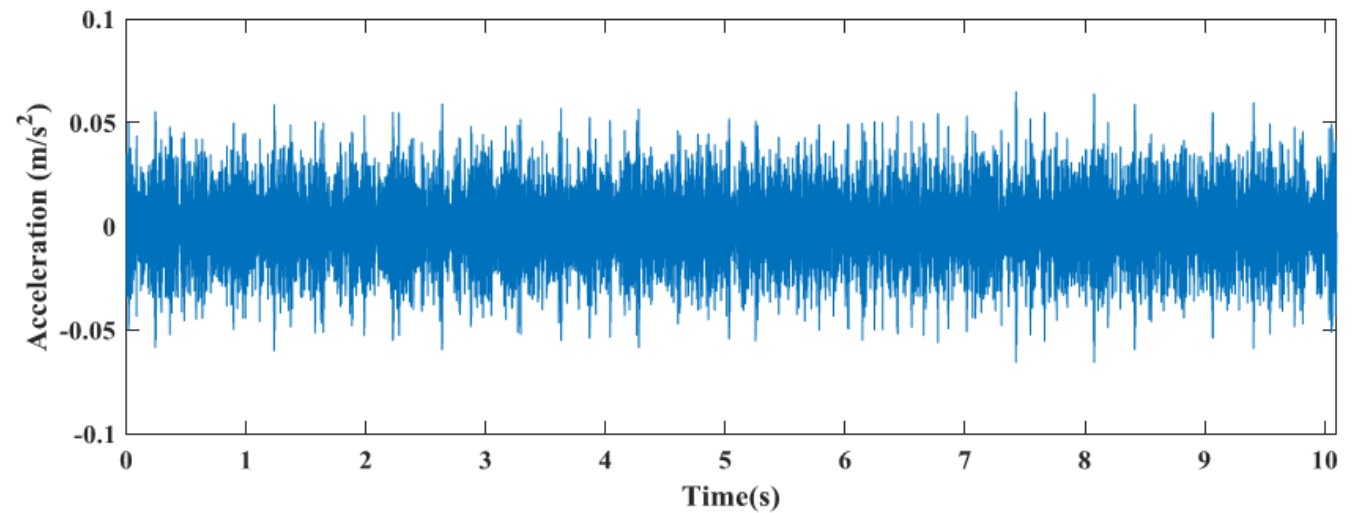
(b) Autogram

- a series of transients is present

(a)



(b)



- **Developed a planetary gear train lumped parameter model**
 - To investigate the gears and bearings interaction in presence of faults
- **Proposed a new enhanced Fast Kurtogram (Autogram)**
 - A method to find the proper frequency band of demodulation for bearing faults diagnosis specially in presence of impulsive noise
- **Two bearing data sets were studied**
 - The results show the improved capability of the Autogram over Fast Kurtogram in dealing with signals with impulsive noise

- **Modify the Model to Take Into Account Flexibility Of Gearboxes Casings and Slippage in Bearings**
- **A new method for REBs diagnosis by considering the whole frequency band**

Publication

Journal Papers

- 1- Moshrefzadeh A, Fasana A “The Autogram: an effective approach for selecting the optimal demodulation band in rolling element bearings diagnosis” *Mechanical Systems and Signal Processing* (submitted)
- 2- Moshrefzadeh A, Fasana A “Planetary gearbox with localized bearings and gears faults: simulation and time/frequency analysis” *Meccanica*, 2017

Conference Paper

- 1- Moshrefzadeh A, Fasana A, Garibaldi L “Using unbiased autocorrelation to enhance kurtogram and envelope analysis results for rolling element bearing diagnostics” *Surveillance 9, International Conference*, 2017

Thanks for
Your
Attention



**POLITECNICO
DI TORINO**